

Proceedings Article

# Single-Sided MPI without Selection Fields: Proof-of-Concept Results

Ege Kor <sup>a,b,\*</sup>, S. Furkan Kahraman <sup>a,†</sup>, Emine Ulku Saritas <sup>a,b</sup>

<sup>a</sup>Department of Electrical and Electronics Engineering, Bilkent University, Ankara, Turkey

<sup>b</sup>National Magnetic Resonance Research Center (UMRAM), Bilkent University, Ankara, Turkey

<sup>†</sup>Shared first authorship

\*Corresponding author, email: [ege.kor@bilkent.edu.tr](mailto:ege.kor@bilkent.edu.tr)

© 2025 Kor *et al.*; licensee Infinite Science Publishing GmbH

This is an Open Access article distributed under the terms of the Creative Commons Attribution License (<http://creativecommons.org/licenses/by/4.0>), which permits unrestricted use, distribution, and reproduction in any medium, provided the original work is properly cited.

## Abstract

In a standard single-sided magnetic particle imaging (MPI) systems, all coils including the selection field coils are positioned on one side of the object to be imaged. In this work, we propose a single-sided MPI system that combines a single-sided magnetic particle spectrometer (MPS) setup and linear movement of the phantom to resolve the magnetic nanoparticle (MNP) distribution along the axis of the system, without the need for selection fields.

## I. Introduction

In single-sided magnetic particle imaging (MPI) systems, all coils including selection field, drive, and receive coils are positioned on one side of the object to be imaged [1]. This configuration removes object size limitations and offers promising applications such as sentinel lymph node imaging [2]. In this work, we propose a single-sided MPI system without selection fields. The proposed setup combines a single-sided magnetic particle spectrometer (MPS) setup with linear movement of the phantom to image spatial distribution of magnetic nanoparticles (MNPs). With proof-of-concept 1D imaging experiments, we demonstrate that the proposed approach successfully resolves the MNP distribution along the axis of the system.

## II. Materials and Methods

Figure 1a shows our in-house single-sided MPS setup, where the region of interest (ROI) for imaging is on one side of the setup along the z-direction. We propose converting this setup to a single-sided MPI system by gradu-

ally moving away the imaged object during signal acquisition. The changes in the received signal due to varying drive field (DF) amplitudes and receive coil sensitivities at different distances are then utilized to resolve the MNP distribution.

Here, we adopt a hybrid system matrix approach that combines measured MNP responses with the measured drive coil and receive coil sensitivities. First, a point source sample is held at a fixed distance from the setup, and calibration measurements are acquired at varying DF amplitudes. Using these measurements and the drive coil sensitivity, the MNP responses that one would get for a point source sample placed at  $N$  different distances from the setup are computed with a grid size of  $\Delta x$ . These responses are further scaled by the receive coil sensitivities at those distances, and placed in a submatrix,  $S_1 \in \mathbb{C}^{H \times N}$ , where  $H$  is the number of harmonics. Here, the columns of  $S_1$  show harmonic responses at distances  $\Delta x[0:N-1]$  to the setup. If an incremental step size of  $\Delta x_s$  is to be applied during imaging, the MNP responses for point sources at distances  $\Delta x_s + \Delta x[0:N-1]$  to the setup can be computed following a similar procedure as described above, to form a submatrix,  $S_2 \in \mathbb{C}^{H \times N}$ . This procedure is then repeated for a total of  $M$  different po-

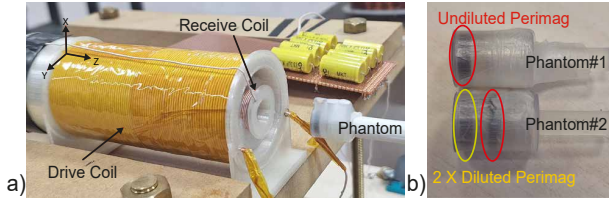


**Figure 1:** (a) Single-sided MPS setup and a phantom attached to the linear actuator. The endpoints of the drive coil and the receive coil are aligned. (b) Imaging phantoms. Phantom #1 contained a single compartment filled with undiluted Perimag. Phantom #2 contained two compartments, filled with 2× diluted and undiluted Perimag, separated by a center-to-center distance of 4.5 mm.

sitions separated by incremental step sizes of  $\Delta x_s$ , and the computed submatrices are concatenated vertically to form the system matrix,  $S \in \mathbb{C}^{HM \times N}$ .

Finally, the measurement vector  $u \in \mathbb{C}^{HM \times 1}$  is acquired, this time by actually stepping the imaging phantom away from the setup in  $M$  steps of step size  $\Delta x_s$  during signal acquisition. The image vector  $c \in \mathbb{R}^{N \times 1}$  that satisfies  $Sc = u$  can then be reconstructed via standard system function reconstruction approaches [3].

### III.1. Imaging Setup and Experiments

Our in-house single-sided MPS setup (see Fig. 1a) is tuned to operate at a DF frequency of 3 kHz. The drive coil has a 44-mm inner diameter and 463  $\mu\text{H}$  inductance. The gradiometric receive coil has a 17-mm inner diameter, with its active section and compensation section aligned with either ends of the drive coil.

Calibration measurements were acquired using a point source phantom prepared using Perimag (Micromod GmbH, Germany) with 8.5 mg Fe/mL undiluted concentration at 170  $\mu\text{L}$ , with DF amplitudes ranging between 1-25 mT with 1 mT increments. The system matrix was then computed as described above for  $\Delta x = \Delta x_s = 0.63$  mm,  $N = 30$ ,  $M = 8$ , and  $H = 4$  (utilizing odd harmonics between  $3^{rd}$ - $9^{th}$  harmonics).

Two different imaging phantoms were prepared (see Fig. 1b): Phantom #1 had a single compartment filled with 170  $\mu\text{L}$  of undiluted Perimag. Phantom #2 had two compartments, filled with 2× diluted and undiluted Perimag at 170  $\mu\text{L}$ , separated by a center-to-center distance of 4.5 mm. The imaging experiments were conducted with a DF amplitude of 25 mT right outside the MPS setup. The imaged phantom was aligned with the surface of the setup and moved with  $\Delta x_s = 0.63$  mm for  $M = 8$  steps using a linear actuator (Velmex BiSlide). Image reconstruction was performed using the regularized Kaczmarz algorithm [3].

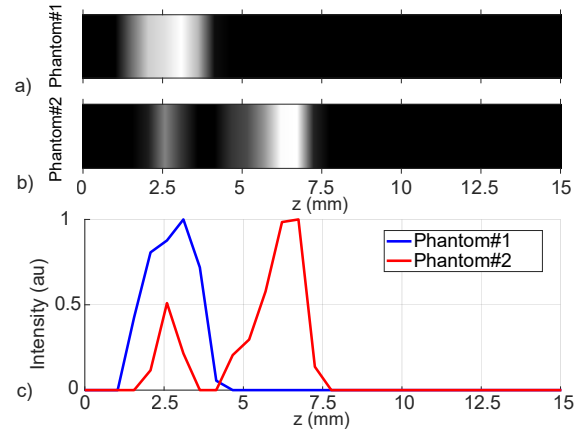


**Figure 2:** 1D images acquired with the proposed single-sided MPI system for Phantom #1 and Phantom #2, displayed in (a-b) concatenated image format and (c) line plots.

## III. Results and Discussion

Figure 2 shows the results of the proof-of-concept 1D imaging experiments performed with the proposed single-sided MPI system. For both imaging phantoms, a reconstruction FOV of 15 mm was utilized. The MPI images for both Phantom #1 and Phantom #2 accurately reflect the concentrations and positions of the MNPs within the phantom. Particularly, for Phantom #2, the concentration ratio of 1:2 and the distance between the two compartments is accurately shown in the image.

In the proposed single-sided MPI system, the imaging depth is mainly restricted by the receive coil sensitivity, which reduces by approximately 43% at 10 mm depth from the surface of the setup. Because the drive coil has a considerably larger diameter than the receive coil, its effect on the imaging depth is less pronounced. Further evaluations on imaging depth, as well as resolution, remain a future work.

## IV. Conclusion

This work proposed a single-sided MPI system without selection fields by combining a single-sided MPS setup with linear movement. The proof-of-concept 1D imaging experiments validate the imaging capability of the system. For this system, the imaging FOV is mainly restricted by the receive coil sensitivity that rapidly falls off away from the system. Scaling the overall system can help improve the imaging FOV.

## Acknowledgments

This work was supported by the Scientific and Technological Research Council of Turkey (TUBITAK 22AG016/23AG005).

## Author's statement

Conflict of interest: Authors state no conflict of interest.

## References

- [1] T. F. Sattel, T. Knopp, S. Biederer, B. Gleich, J. Weizenecker, J. Borgert, and T. M. Buzug. Single-sided device for magnetic particle imaging. *Journal of Physics D: Applied Physics*, 42(2):022001, 2008, doi:[10.1088/0022-3727/42/2/022001](https://doi.org/10.1088/0022-3727/42/2/022001).
- [2] T. F. Sattel, M. Erbe, S. Biederer, T. Knopp, D. Finas, K. Diedrich, K. Lüdtké-Buzug, J. Borgert, and T. M. Buzug. Single-sided magnetic particle imaging device for the sentinel lymph node biopsy scenario, in *Medical Imaging 2012: Biomedical Applications in Molecular, Structural, and Functional Imaging*, R. C. Molthen and J. B. Weaver, Eds., International Society for Optics and Photonics, 8317, 83170S, SPIE, 2012. doi:[10.1117/12.912733](https://doi.org/10.1117/12.912733).
- [3] T. Knopp, J. Rahmer, T. F. Sattel, S. Biederer, J. Weizenecker, B. Gleich, J. Borgert, and T. M. Buzug. Weighted iterative reconstruction for magnetic particle imaging. *Physics in Medicine & Biology*, 55(6):1577, 2010, doi:[10.1088/0031-9155/55/6/003](https://doi.org/10.1088/0031-9155/55/6/003).